

Transactivator of transcription (TAT) peptide–chitosan functionalized multiwalled carbon nanotubes as a potential drug delivery vehicle for cancer therapy

Xia Dong
Lanxia Liu
Dunwan Zhu
Hailing Zhang
Xigang Leng

Laboratory of Bioengineering,
Institute of Biomedical Engineering,
Chinese Academy of Medical Sciences
and Peking Union Medical College,
Tianjin Key Laboratory of Biomedical
Materials, Tianjin, People's Republic
of China

Abstract: Carbon nanotube (CNT)-based drug delivery vehicles might find great potential in cancer therapy via the combination of chemotherapy with photothermal therapy due to the strong optical absorbance of CNTs in the near-infrared region. However, the application of CNTs in cancer therapy was considerably constrained by their lack of solubility in aqueous medium, as well as the cytotoxicity caused by their hydrophobic surface. Intracellular delivery efficiency is another factor determining the application potential of CNTs in cancer therapy. In the present study, low-molecular-weight chitosan conjugated with transactivator of transcription (TAT) peptide was used for noncovalent functionalization of multiwalled carbon nanotubes (MWCNTs), aiming at providing a more efficient drug delivery vehicle for cancer therapy. The TAT–chitosan-conjugated MWCNTs (MWCNTs-TC) were further investigated for their water solubility, cytotoxicity, cell-penetrating capability, and accumulation in tumor. It was found that MWCNTs-TC were essentially nontoxic with satisfying water solubility, and they were more efficient in terms of cancer-targeted intracellular transport both *in vitro* and *in vivo* as compared with chitosan-modified MWCNTs (MWCNTs-CS), suggesting the great application potential of MWCNTs-TC in cancer therapy.

Keywords: carbon nanotube, TAT, chitosan, drug delivery

Introduction

Carbon nanotubes (CNTs) have been attracting increasing attention as potential delivery vehicles for intracellular transport of nucleic acids, proteins, and drug molecules due to their unique properties such as their high surface area-to-volume ratio.^{1–5} One of the intrinsic properties of CNTs is their strong optical absorbance in the near-infrared (NIR) region, which was reported to enhance thermal destruction of cancerous cells during NIR laser irradiation, revealing the great application potential of CNT-based drug delivery vehicles in cancer therapy by combining chemotherapy with physical therapy such as photothermal therapy.^{6–9}

However, the application of CNTs in cancer therapy was considerably constrained by their lack of solubility in aqueous medium, as well as the cytotoxicity caused by their hydrophobic surface. To resolve this problem, a number of procedures were designed to attach appropriate molecules on the CNT surface, a process called functionalization, to increase their solubility or dispersion and lower their toxicity. Further chemical reactions with various functional molecules including therapeutic agents or targeting moieties have been demonstrated to significantly improve their performance as drug/gene delivery vehicles.^{10–14}

Correspondence: Xigang Leng
Laboratory of Bioengineering, Institute
of Biomedical Engineering, Chinese
Academy of Medical Sciences and Peking
Union Medical College, 236 Baidi Road,
Nankai District, Tianjin 300192, People's
Republic of China
Email lengxyky@163.com

Functionalization of CNTs could be realized by either a covalent or noncovalent approach. Covalent functionalization is usually governed by oxidation of CNTs with strong acids which generates COOH or OH on the CNT surface.¹⁵ CNTs can also noncovalently interact with various molecules through weak interactions such as surface adsorption, π - π stacking, electrostatic interactions, hydrogen bonding or van der Waals force.¹⁶⁻¹⁸ Since covalent functionalization would definitely alter the electronic structure of CNTs, and hence might potentially affect their physical properties, noncovalent functionalization is more attractive as it offers the facility of associating functional groups with the CNT surface without changing the system of the grapheme lattice, and thus not modifying their electrical or physical properties. A variety of biomolecules, polymers, and surfactants have been utilized for noncovalent functionalization of CNTs.¹⁹⁻²¹

Chitosan (CS), a cationic polysaccharide derived from chitin, has been intensively investigated as a drug/gene delivery vehicle and tissue engineering scaffold, owing to its excellent biocompatibility, biodegradability, and low immunogenicity.²²⁻²⁵ Previous reports showed that the functionalization of CNTs with CS through surface adsorption could increase their dispersibility in the solution.²⁶⁻²⁷ A novel immunologically modified nanotube system invented by Zhou et al²⁸ using glycated CS-modified single-walled CNTs resulted in highly effective tumor suppression in animal tumor models, with complete tumor regression and long-term survival in many cases.

The capability of efficiently penetrating into cells is one of the prerequisites for the drug/gene delivery vehicles. Transactivator of transcription (TAT) peptide, a widely accepted cell-penetrating peptide that can penetrate across the cell membrane in less than 1 minute, has been successfully utilized to modify several polymers to enhance their cell-penetrating capability.^{29,30} In the present study, low-molecular-weight CS (LMWC) conjugated with TAT peptide was used for noncovalent functionalization of multiwalled CNTs (MWCNTs), aiming at providing a more efficient drug delivery vehicle for cancer therapy. The TAT-CS-conjugated MWCNTs (MWCNTs-TC) were further investigated for their water solubility, cytotoxicity, cell-penetrating capability, and in vivo accumulation in the target tumor tissues.

Experimental section

Materials

Pristine MWCNTs (p-MWCNTs) (purity >98%, 0.5–2 μ m in length with a diameter less than 8 nm) were purchased from Chengdu Organic Chemicals Co., Ltd. (Sichuan, People's Republic of China). LMWC (molecular weight of 5,000–8,000 Da; degree of deacetylation of 90%) was

obtained from Golden-Shell Biochemical Co., Ltd. (Yuhuan, Zhejiang, People's Republic of China). Fetal bovine serum (FBS) was provided by Gibco® (Thermo Fisher Scientific, Waltham, MA, USA). TAT peptide with the amino acid sequence of YGRKKRRQRRR was synthesized by SBS Genetech Co., Ltd (Beijing, People's Republic of China).

Synthesis and characterization of TAT-CS conjugates

TAT-CS conjugates (TC) was synthesized by covalently coupling the TAT peptide with LMWC using Traut's Reagent as the sulfhydryl agent and *N*-succinimidyl-3-(2-pyridyldithio)propionate (SPDP) (Thermo Fisher Scientific) as the linking agent. The substitution degree of TC was estimated by proton nuclear magnetic resonance (¹H-NMR) spectroscopic analysis (Varian Inova 500 MHz; Varian Medical Systems Inc., Palo Alto, CA, USA).

Preparation and characterization of MWCNTs-TC and MWCNTs-CS

A total of 0.2 mg p-MWCNTs were mixed with 500 μ L of a TC or CS solution at different concentrations (0.4–4 mg/mL); the mixture was sonicated for 40 minutes at room temperature, followed by filtrating through the Millipore filters with a molecular weight cut-off of 10 KDa (Merck Millipore, Billerica, MA, USA) to remove the excessive TC or CS. The resultant MWCNTs-TC or MWCNTs-CS were characterized with an infrared spectroscope (Nicolet 2000; Thermo Fisher Scientific) and ¹H-NMR spectroscopic analysis (Varian Inova 500 MHz). Raman spectra were collected using a Renishaw in a Via Raman spectrometer (Renishaw PLC, Gloucestershire, UK) with an excitation wavelength at 532 nm. MWCNTs were deposited on glass slides and detailed scans were performed in the 1,000–2,000 cm^{-1} range. The weight percentage of TC or CS coated on the MWCNTs surface was determined using a Thermogravimetric Analyzer (Q500; TA instruments, New Castle, DE, USA). To determine the dispersal capacity of CS or TC for MWCNTs and the stability of the CNT suspension, p-MWCNTs, MWCNTs-CS, or MWCNTs-TC were prepared at a mass ratio of 10:1 and stored at 4°C for 2 months. After that, the solution state was observed, and the size and surface morphology of the CNTs were analyzed by transmission electron microscopy (JEM-1010; JEOL, Tokyo, Japan). The zeta potential was measured with a Zetasizer Nano-ZS instrument (Malvern Instruments, Malvern, UK).

Cell culture

Human breast cancer cell line MD-MBA-231 cells were cultured in Leibovitz's L-15 medium (Gibco®, Thermo

Fisher Scientific), murine fibroblast cell line L929 cells were cultured in Roswell Park Memorial Institute 1640 medium (HyClone Laboratories, Inc., Logan, UT, USA), and human umbilical vein endothelial cells (HUVECs) were cultured in endothelial cell medium (ScienCell Research Laboratories, Carlsbad, CA, USA), with all the medium being supplemented with 10% FBS, penicillin (100 units/mL), and streptomycin (100 mg/mL).

Cell viability evaluation

The viability of MD-MBA-231, L929, or HUVEC cells after 24 hours of incubation with different concentrations of MWCNTs-TC, MWCNTs-CS, or p-MWCNTs (1 $\mu\text{g/mL}$, 2.5 $\mu\text{g/mL}$, 5 $\mu\text{g/mL}$, 10 $\mu\text{g/mL}$, and 20 $\mu\text{g/mL}$, respectively) was assessed with Cell Counting Kit-8 (Dojindo Molecular Technologies, Inc., Kumamoto, Japan) according to the manufacturer's instructions, with untreated cells serving as the experimental control. The optical absorbance at 450 nm was measured using a microplate reader (The Varioskan™ Flash; Thermo Fisher Scientific). Six wells were measured for each test.

Cellular uptake observation

MWCNTs-TC or MWCNTs-CS were fluorescently labeled for monitoring the cellular uptake of the CNTs. Briefly, 2 μL of Alexa Fluor® 488 Carboxylic Acid (Thermo Fisher Scientific) dissolved in 100 μL of dimethyl sulfoxide was mixed with 500 μL of a MWCNTs-TC or MWCNTs-CS solution, followed by filtration through the Millipore filters with a molecular weight cut-off of 10 kDa to remove the excessive fluoresceins. To investigate the cellular uptake of the CNTs, MD-MBA-231 cells were coincubated with the labeled MWCNTs-TC or MWCNTs-CS (5 $\mu\text{g/mL}$) for 24 hours. The cells were then washed three times with phosphate buffered saline (PBS) and fixed in 4% paraformaldehyde for 10 minutes, followed by labeling the intracellular microtubules with Alexa Fluor® 555 provided in the Tubulin Tracker Red Kit (Thermo Fisher Scientific) and subsequent staining of the nucleus with 4',6-diamidino-2-phenylindole dihydrochloride (DAPI) (Beyotime Institute of Biotechnology, Shanghai, People's Republic of China). Internalization of MWCNTs-TC and MWCNTs-CS was observed with a laser confocal microscope (LSM710; Carl Zeiss Meditec AG, Jena, Germany). For the measurement of the cellular uptake rate, the cells were harvested by centrifugation and resuspended in PBS followed by three times of washing before being applied to flow cytometry (FACSCalibur; BD Biosciences, San Jose, CA, USA).

In vivo distribution of CNTs in tumor-bearing mice

All animal procedures were conducted following the protocol approved by the Institutional Laboratory Animal Ethics Committee, and all animal experiments were performed in compliance with the Guiding Principles for the Care and Use of Laboratory Animals, Peking Union Medical College, People's Republic of China. MD-MBA-231 cells (1×10^6) in 0.1 mL of normal saline (NS) were injected into the armpit region of Balb/c nude mice (6 weeks, male, from Peking Union Medical College, Beijing, People's Republic of China). When the volume of tumors reached to $\sim 100 \text{ mm}^3$, the MWCNTs-TC or MWCNTs-CS labeled with Alexa Fluor® 700 N-Hydroxysuccinimide Ester (Thermo Fisher Scientific), according to the method described in "Cellular uptake observation" were intravenously injected into tumor-bearing mice with NS-treated mice as the negative control (six mice per group). Living animal imaging was conducted at 24 hours, 48 hours, and 72 hours after CNTs administration. At the end of each imaging, one mouse from each group was sacrificed and the heart, liver, spleen, lung, and kidney, as well as the tumor tissues, were excised and imaged using a CRI imaging system (Maestro EX; Cambridge Research & Instrumentation Inc., Woburn, MA, USA) with an exposure time of 200 ms, and the images were analyzed using the CRI Analysis Software.

Statistical analysis

Data were presented as the mean of six individual observations with the standard deviation. The statistical analysis was performed using the Bonferroni *t*-test. Statistical significance was determined at $P < 0.05$.

Results

¹H-NMR spectroscopic analysis

¹H-NMR spectroscopic analysis was conducted to characterize TC and CS, and the results are shown in Figure 1. The $\delta = 3.299\text{--}4.125$ ppm attributed to the protons of $-\text{CH}_2-$ in CS, the $\delta = 1.276\text{--}1.574$ ppm and $\delta = 0.460\text{--}0.476$ ppm attributed to $-\text{NH}_2\text{-CH}_2$ of spermine protons in the TAT peptide, and the $\delta = 6.534\text{--}7.251$ ppm attributed to the methine proton of the tyrosine in TAT were observed, indicating the successful conjugation of TAT peptides with the primary amino groups of CS. It was estimated that the substitution degree of TC was about 4.1%, according to the area ratio above the peak. No significant change was observed in the ¹H-NMR of TC or CS coated onto MWCNTs.

Raman spectroscopic analysis

Figure 2 shows the Raman spectra of the p-MWCNTs, MWCNTs-CS, and MWCNTs-TC. Each spectrum consists of

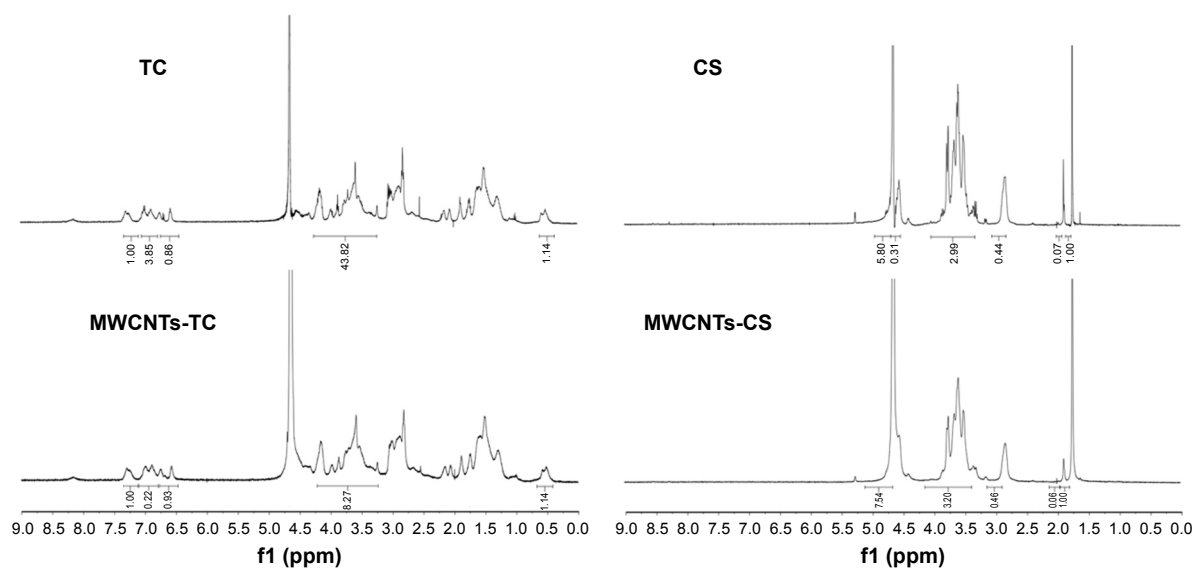


Figure 1 $^1\text{H-NMR}$ spectra analysis.

Abbreviations: TC, transactivator of transcription–chitosan conjugate; CS, chitosan; MWCNTs-TC, transactivator of transcription–chitosan-conjugated multiwalled carbon nanotubes; MWCNTs-CS, chitosan-conjugated multiwalled carbon nanotubes; $^1\text{H-NMR}$, proton nuclear magnetic resonance.

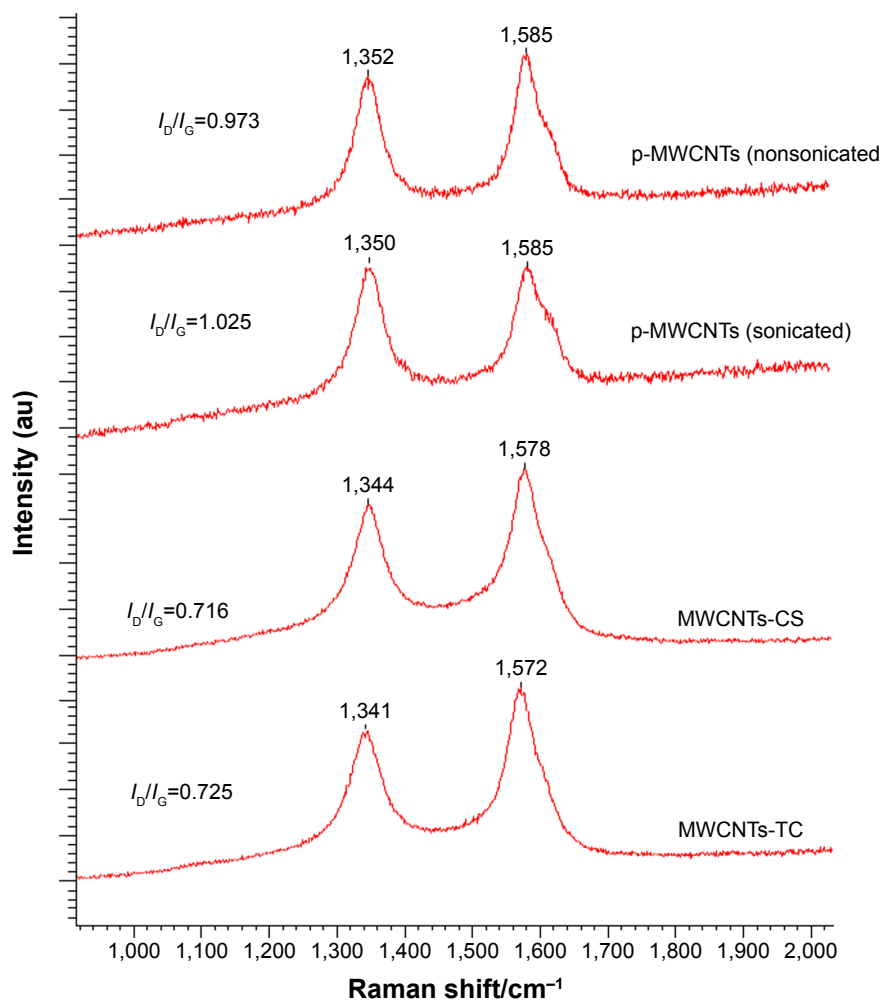


Figure 2 Raman spectra of the p-MWCNTs, MWCNTs-CS, and MWCNTs-TC.

Abbreviations: I_D/I_G , peak intensity ratio of D and G band; MWCNTs, multiwalled carbon nanotubes; MWCNTs-CS, chitosan-conjugated multiwalled carbon nanotubes; MWCNTs-TC, transactivator of transcription–chitosan-conjugated multiwalled carbon nanotubes; p-MWCNTs, pristine multiwalled carbon nanotubes.

a D-band ($1,341\text{--}1,352\text{ cm}^{-1}$) and a G-band ($1,572\text{--}1,585\text{ cm}^{-1}$). The D band is attributed to the disordered species, while the G band is ascribed to the skeletal stretching vibration mode of the graphitic component (SP² bonding). The I_D/I_G (peak intensity) ratio for the respective D- and G-band is commonly used for qualitative analysis regarding the formation of defects in CNTs. The result demonstrated that the I_D/I_G ratio had a slight increase for p-MWCNTs after sonicating, which indicated that sonication caused some slight changes. It is interesting to note that modification of the CNTs with CS or TC led to a decreasing I_D/I_G ratio, while there was no significant difference between MWCNTs-CS and MWCNTs-TC.

Characterization of MWCNTs-TC and MWCNTs-CS

The stability of the p-MWCNTs, MWCNTs-CS, or MWCNTs-TC suspensions was observed by visual inspection and transmission electron microscopic analysis. As illustrated in Figure 3, the visual inspection results demonstrated that both the MWCNTs-CS and MWCNTs-TC suspension remained highly stable even after storage at 4°C for 2 months, while the p-MWCNTs aggregated very soon after preparation. Transmission electron microscopic observation showed that MWCNTs-CS and MWCNTs-TC were better dispersed than the p-MWCNTs, but no obvious morphological difference was found among the three types of MWCNTs.

Figure 4 showed the results of Fourier transform infrared spectroscopic analysis, which revealed that the characteristic absorption peak of the amide was at $1,403.7\text{ cm}^{-1}$ and $1,659\text{ cm}^{-1}$ for the CS molecule on MWCNTs-CS, while in the MWCNTs-TC, the intensity of the characteristic absorption peak of the amide at $1,536.2\text{ cm}^{-1}$ was decreased and the secondary amine bond at $1,656.7\text{ cm}^{-1}$ was increased; the characteristic peaks of the benzene ring in tyrosine attributed to the grafted TAT peptide segment was 801.4 cm^{-1} . All those data indicated the successful modification of MWCNTs with TC or CS.

Figure 5 shows the Thermogravimetric Analyzer results of MWCNTs-TC and MWCNTs-CS, which revealed obvious weight loss in the temperature range of 300°C–400°C for MWCNTs-TC and MWCNTs-CS as compared with p-MWCNTs, and the amount of CS and TC coated on MWCNTs calculated from the difference in weight loss were 58.54 wt% and 59.79 wt%, respectively.

As shown in Figure 6, the average zeta potential was 47.7 ± 1.96 for MWCNTs-TC and 46.1 ± 1.83 for MWCNTs-CS, which was much higher than that for p-MWCNTs (13 ± 1.32), indicating that coating of the positively-charged CS or TC elevated the zeta potential of the MWCNTs.

Cytotoxicity assessment of MWCNTs-TC, MWCNTs-CS, and p-MWCNTs

The toxicity of p-MWCNTs, MWCNTs-TC, or MWCNTs-CS against two typical normal cell lines (HUVEC, L929) and one breast cancer cell line (MD-MBA-231) was assessed by the Cell Counting Kit-8 assay. As shown in Figure 7, both MWCNTs-TC and MWCNTs-CS were less toxic against the three types of cells as compared with p-MWCNTs, and MWCNTs-CS was the least cytotoxic. Also interesting was that the CNTs tested were more cytotoxic against the normal cell lines (HUVEC and L929) than against the tumor cells.

Cellular uptake of MWCNTs-TC and MWCNTs-CS

Internalization of MWCNTs-TC or MWCNTs-CS into MD-MBA-231 cells was observed with laser confocal microscope and it showed that both MWCNTs-TC and MWCNTs-CS could efficiently enter the tumor cells, and they mainly accumulated in the cytoplasm (Figure 8). Flow cytometric analysis demonstrated that the cellular uptake rate of MWCNTs-TC were moderately higher ($84.69\%\pm 5.03\%$) than that of MWCNTs-CS ($72.85\%\pm 4.95\%$). Particularly important was the finding that the fluorescent intensity in the MD-MBA-231

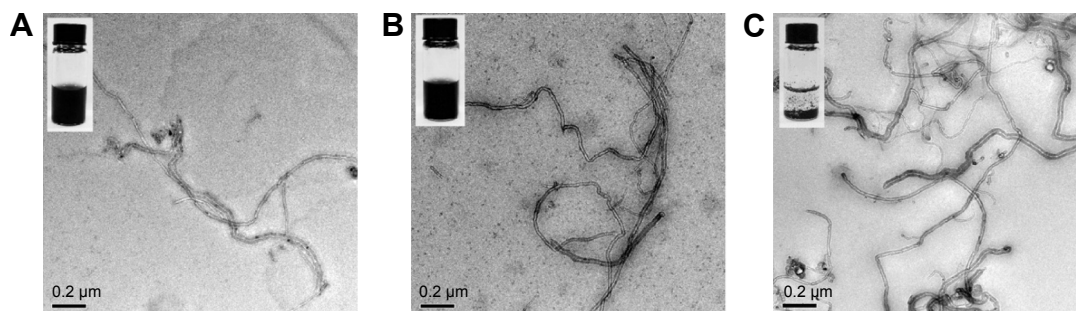


Figure 3 Transmission electron microscopic images of MWCNTs-TC, MWCNTs-CS, and p-MWCNTs after storage at 4°C for 2 months. **Notes:** (A) MWCNTs-TC, (B) MWCNTs-CS, and (C) p-MWCNTs. The insets show a photo of MWCNTs-TC, MWCNTs-CS, and p-MWCNTs solution; respectively. **Abbreviations:** MWCNTs-TC, transactivator of transcription–chitosan-conjugated multiwalled carbon nanotubes; MWCNTs-CS, chitosan-conjugated multiwalled carbon nanotubes; p-MWCNTs, pristine multiwalled carbon nanotubes.

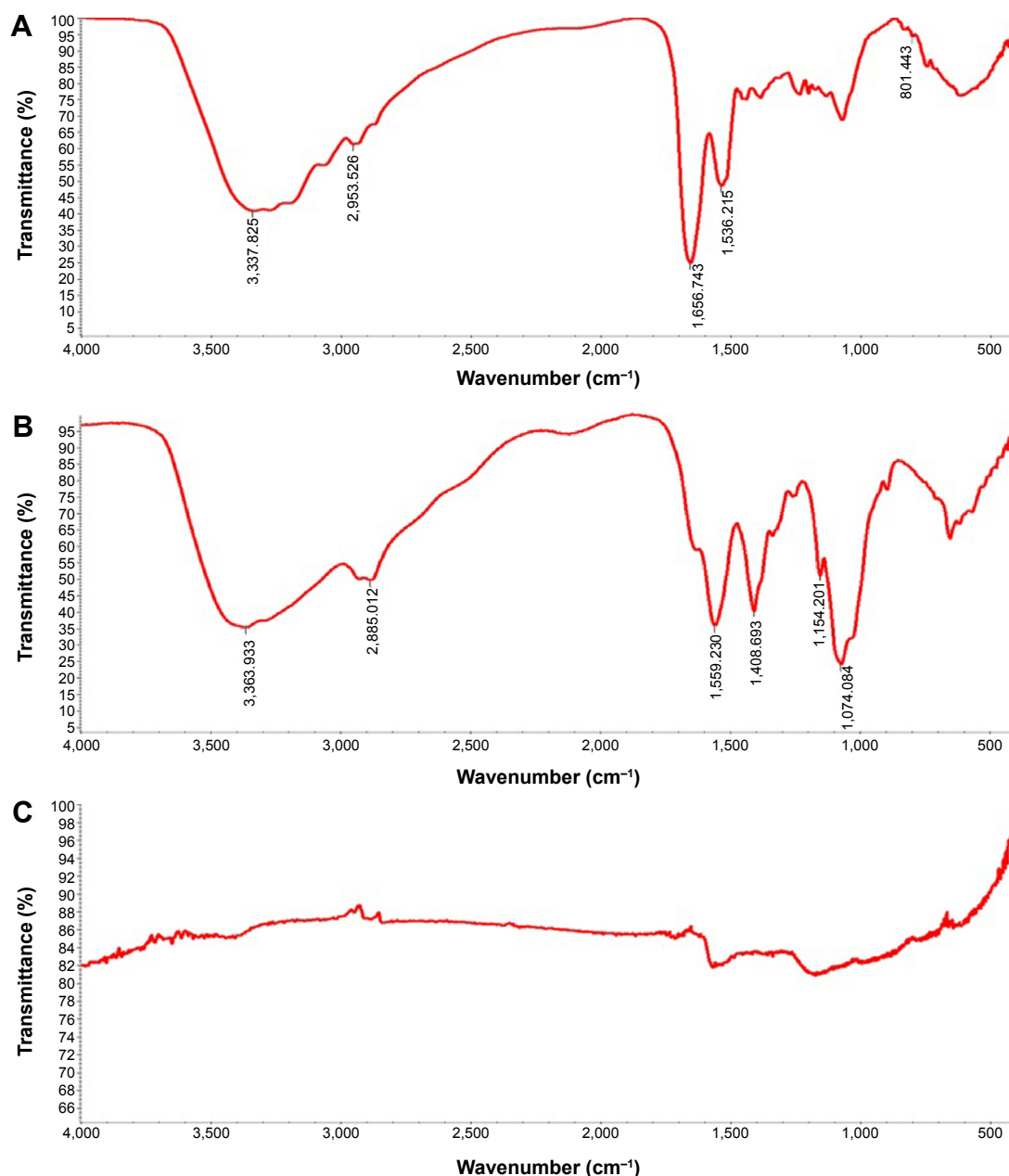


Figure 4 FTIR spectra of MWCNTs-TC, MWCNTs-CS, and p-MWCNTs.

Notes: (A) MWCNTs-TC, (B) MWCNTs-CS, and (C) p-MWCNTs.

Abbreviations: FTIR, Fourier transform infrared spectroscopy; MWCNTs-TC, transactivator of transcription–chitosan-conjugated multiwalled carbon nanotubes; MWCNTs-CS, chitosan-conjugated multiwalled carbon nanotubes; p-MWCNTs, pristine multiwalled carbon nanotubes.

cells incubated with MWCNTs-TC was about 25 times higher than that in the cells incubated with MWCNTs-CS, revealing that more MWCNTs-TC were taken up by each cell as compared with MWCNTs-CS (Figure 9).

In vivo distribution study

Living animal imaging on breast cancer-bearing mice was conducted to investigate the in vivo distribution of intravenously administered fluorescent MWCNTs-TC or MWCNTs-CS, and the results are presented in Figure 10. In the MWCNTs-TC group, strong fluorescence in the tumor tissues and kidney was

observed at 24 hours after injection, and visible fluorescence was still found in the tumor tissues and kidney at 48 hours and 72 hours after the injection, although the fluorescent intensity gradually attenuated with time. In the MWCNTs-CS group, visible fluorescence was only observed in the kidney at 24 hours and 48 hours after the injection, which diminished at 72 hours after the injection. No visible fluorescence was observed anywhere at any time in the NS-treated mice.

Direct imaging on the harvested tissues was conducted to further elucidate the in vivo distribution profiles of the CNTs. As illustrated in Figure 11, it was demonstrated that higher

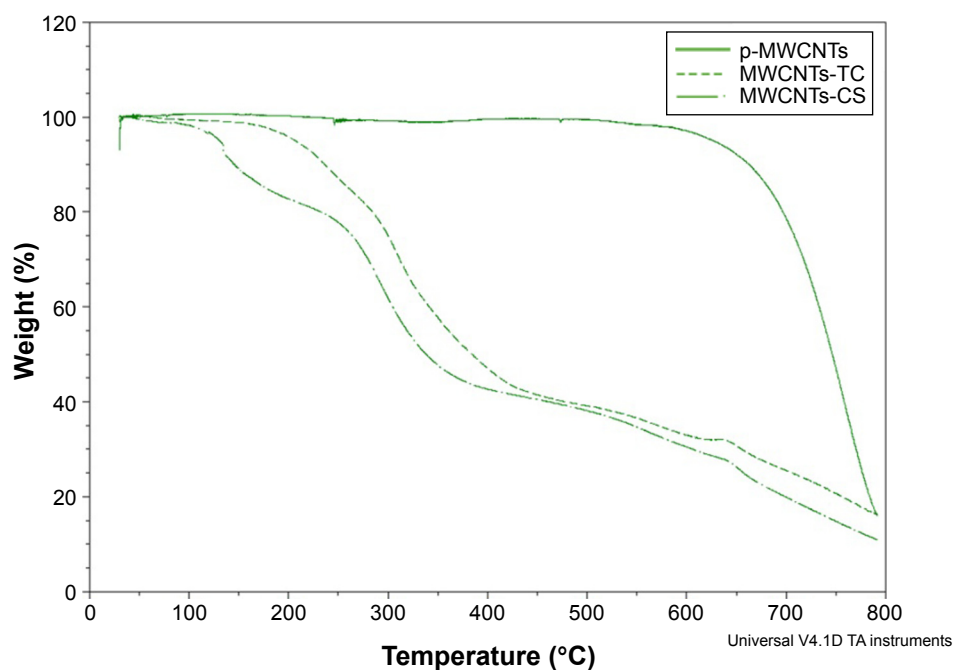


Figure 5 Analysis of p-MWCNTs, MWCNTs-TC, and MWCNTs-CS by TGA.

Abbreviations: MWCNTs, multiwalled carbon nanotubes; MWCNTs-TC, transactivator of transcription–chitosan-conjugated multiwalled carbon nanotubes; MWCNTs-CS, chitosan-conjugated multiwalled carbon nanotubes; p-MWCNTs, pristine multiwalled carbon nanotubes; TGA, Thermogravimetric Analyzer.

amounts of MWCNTs-TC were distributed in the tumor, liver, and lung, as compared with that of the MWCNTs-CS at 24 hours and 48 hours after administration. Obvious kidney distribution was observed in both the MWCNTs-TC group and the MWCNTs-CS group, and no dramatic difference was found between the two groups. No heart and spleen distribution was found in either the MWCNTs-CS or MWCNTs-TC group.

Discussion

The major goal of the present study is to develop a more efficient CNT-based drug delivery vehicle, in hopes of providing a potential tool for combining chemotherapy with photothermal therapy to enhance the therapeutic effects for cancer. To improve the water solubility and biocompatibility of the MWCNTs, which are the two major constraints limiting their medical application, MWCNTs were functionalized with TC or CS, and these functionalized MWCNTs were studied in terms of their solubility, biocompatibility, cellular uptake, as well as *in vivo* distribution in breast cancer-bearing mice.

The amount of polymer coated onto MWCNTs was a key factor determining their dispersability in aqueous solution. Therefore, the water dispersability of MWCNTs-TC prepared at different TC/MWCNTs ratios (w/w) was observed, and it was found that MWCNTs-TC with a TC/MWCNTs (w/w) ratio of 10:1 was most water soluble and stable. More

importantly is that coating with TC or CS led to no obvious morphological change in the MWCNTs, suggesting that TC might be a suitable molecule for the noncovalent functionalization of CNTs.

To efficiently penetrate into the target cells is one of the prerequisites for the realization of the expected functions of CNTs. We first observed the internalization of the CNTs with laser confocal microscope, which showed that both MWCNTs-TC and MWCNTs-CS could efficiently enter the breast cancer cells and that they mainly accumulated in the cytoplasm, which was consistent with the previous report.²⁰ Further analysis by flow cytometry demonstrated that MWCNTs-TC were taken up by almost 85% of the cells in contact, which is moderately higher than the amount of MWCNTs-CS (72.85%±4.95%). Particularly important was the finding that the amount of MWCNTs-TC in each cell was about 25 times higher than that of MWCNTs-CS, confirming the superiority of MWCNTs-TC over MWCNTs-CS in terms of their intracellular delivery efficiency, which is probably due to the presence of TAT peptide in the former.

The *in vivo* distribution of MWCNTs-TC and MWCNTs-CS in breast cancer-bearing mice was investigated by both living animal imaging and direct imaging on the tissues and organs harvested from the mice. Living animal imaging revealed that clearly visible MWCNTs-TC accumulation in tumor tissues was observed with decreasing amounts of

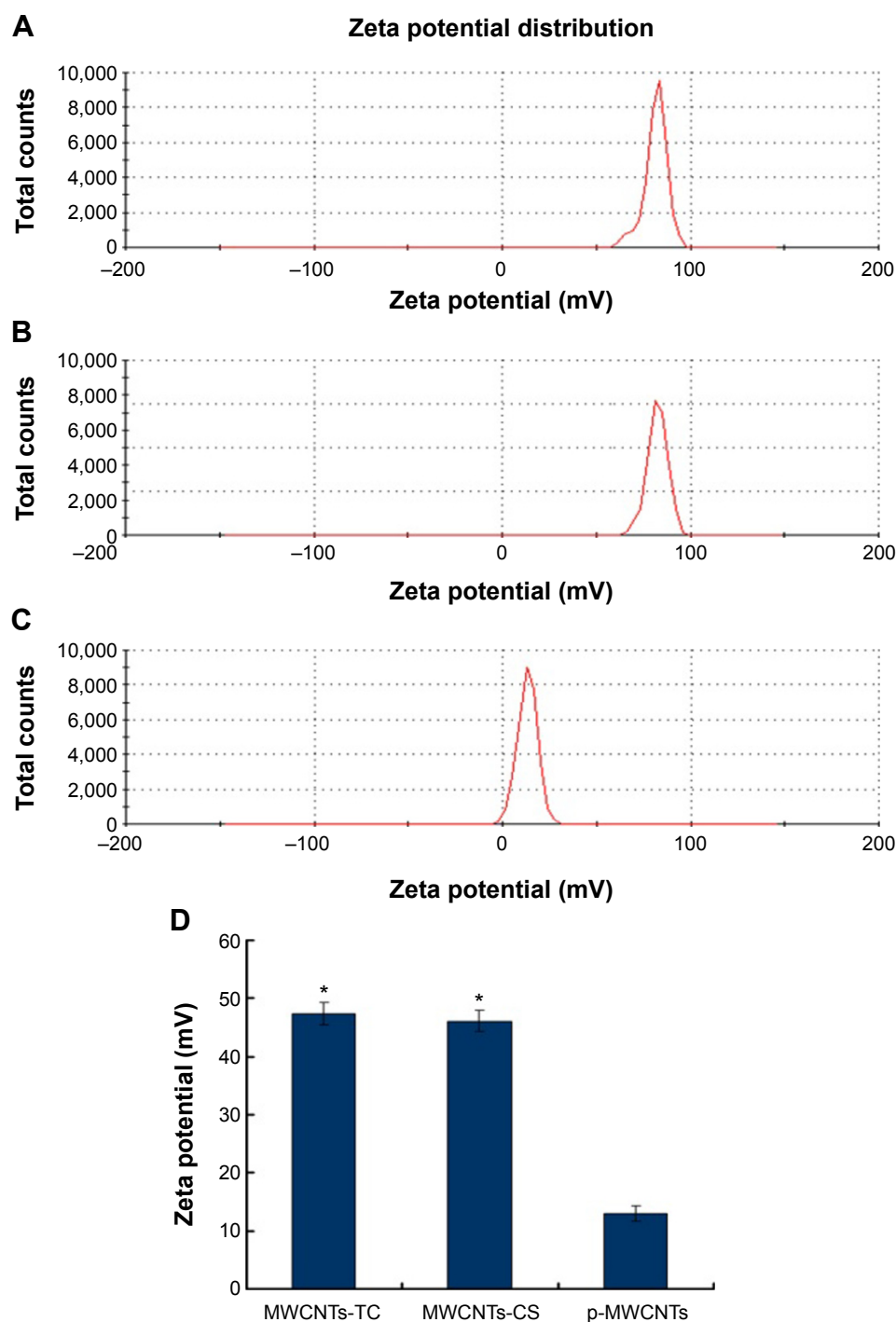


Figure 6 Zeta potential of MWCNTs-TC, MWCNTs-CS, and p-MWCNTs.

Notes: (A) MWCNTs-TC, (B) MWCNTs-CS, and (C) p-MWCNTs. (D) represents the statistical analysis of Zeta potential for three groups of MWCNTs. * $P < 0.05$ versus p-MWCNTs.

Abbreviations: MWCNTs-TC, transactivator of transcription–chitosan-conjugated multiwalled carbon nanotubes; MWCNTs-CS, chitosan-conjugated multiwalled carbon nanotubes; MWCNTs, multiwalled carbon nanotubes; p-MWCNTs, pristine multiwalled carbon nanotubes.

time, whereas no tumor accumulation was found in either the MWCNTs-CS- or NS-treated mice during the observation period of 72 hours. Direct imaging on the harvested tissue or organs would provide more accurate and precise information as compared with living animal imaging technology due to

its limited detection depth, and it was applied in the present study to further elucidate the *in vivo* distribution profiles of the CNTs. It was found that more MWCNTs-TC were distributed in the tumor as compared with MWCNTs-CS, which might be attributed to the presence of TAT in the

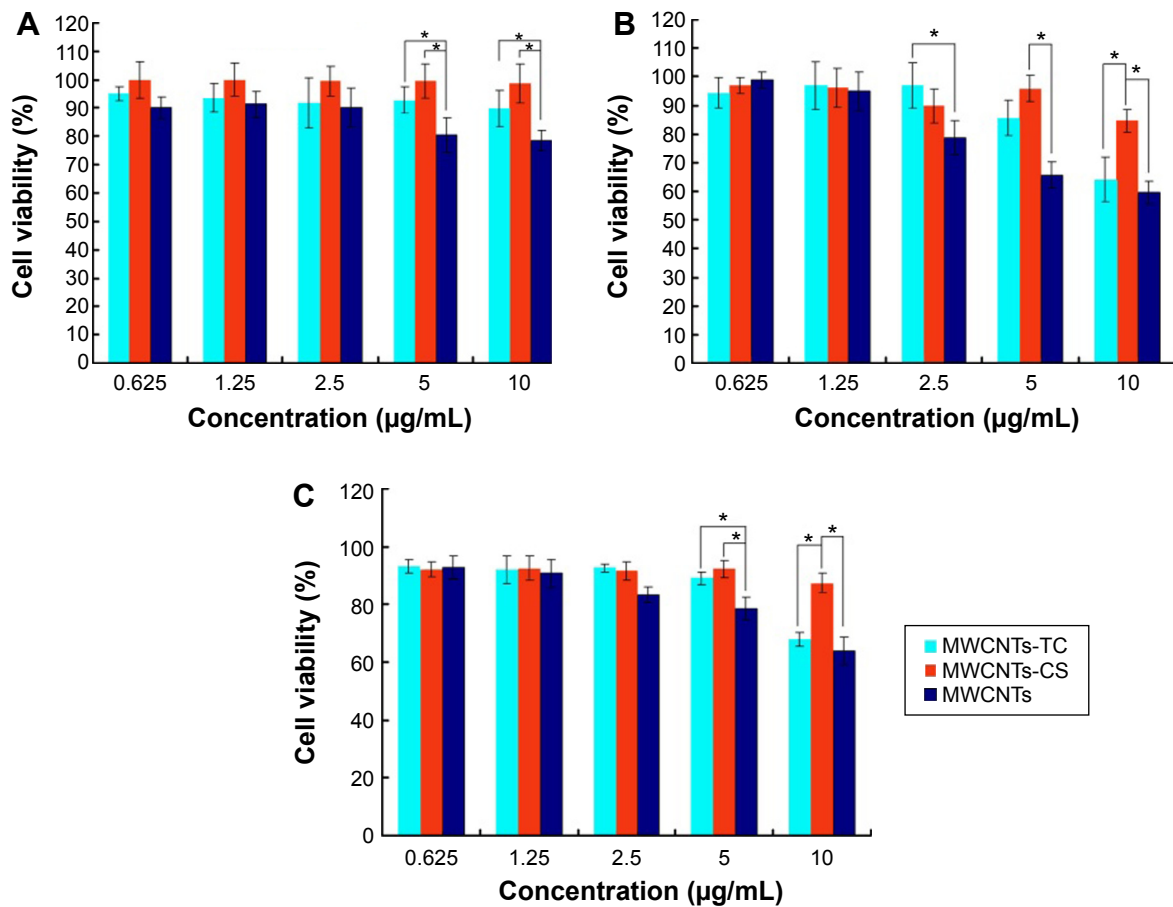


Figure 7 Toxicity of MWCNTs-TC or MWCNTs-CS against MD-MBA-231, HUVEC, and L929.

Notes: (A) MD-MBA-231; (B) HUVEC; and (C) L929. * $P < 0.05$.

Abbreviations: MWCNTs-TC, transactivator of transcription–chitosan-conjugated multiwalled carbon nanotubes; MWCNTs-CS, chitosan-conjugated multiwalled carbon nanotubes; MWCNTs, multiwalled carbon nanotubes; HUVEC, human umbilical vein endothelial cell.

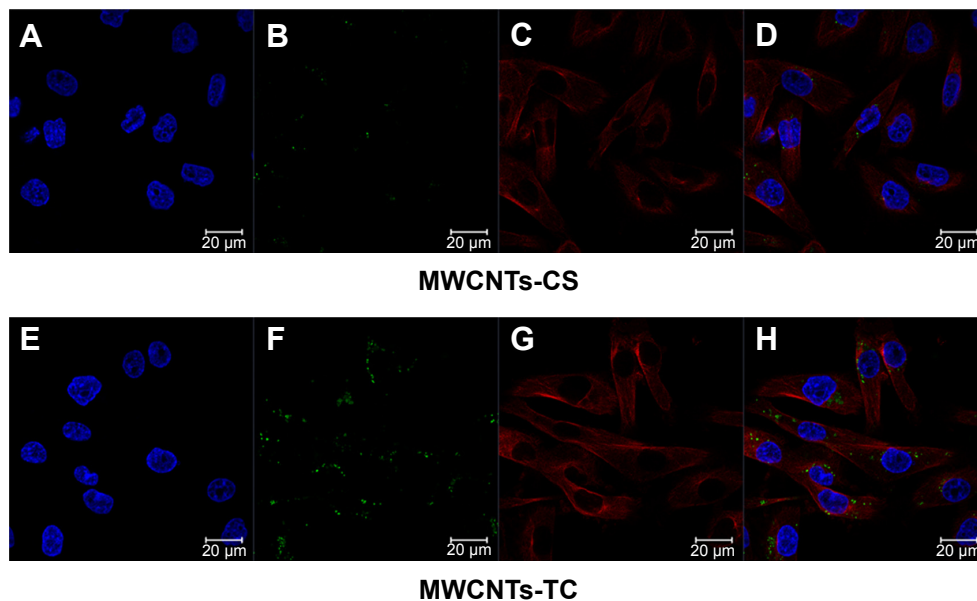


Figure 8 Laser confocal microscopy for MWCNTs-TC and MWCNTs-CS.

Notes: (A and E) Cell nucleus (DAPI); (B and F) MWCNTs (Alexa Fluor[®] 488); (C and G) microtubules (Alexa Fluor[®] 555); and (D and H) merge.

Abbreviations: MWCNTs-CS, chitosan-conjugated multiwalled carbon nanotubes; MWCNTs-TC, transactivator of transcription–chitosan-conjugated multiwalled carbon nanotubes; DAPI, 4',6-diamidino-2-phenylindole dihydrochloride; MWCNTs, multiwalled carbon nanotubes.

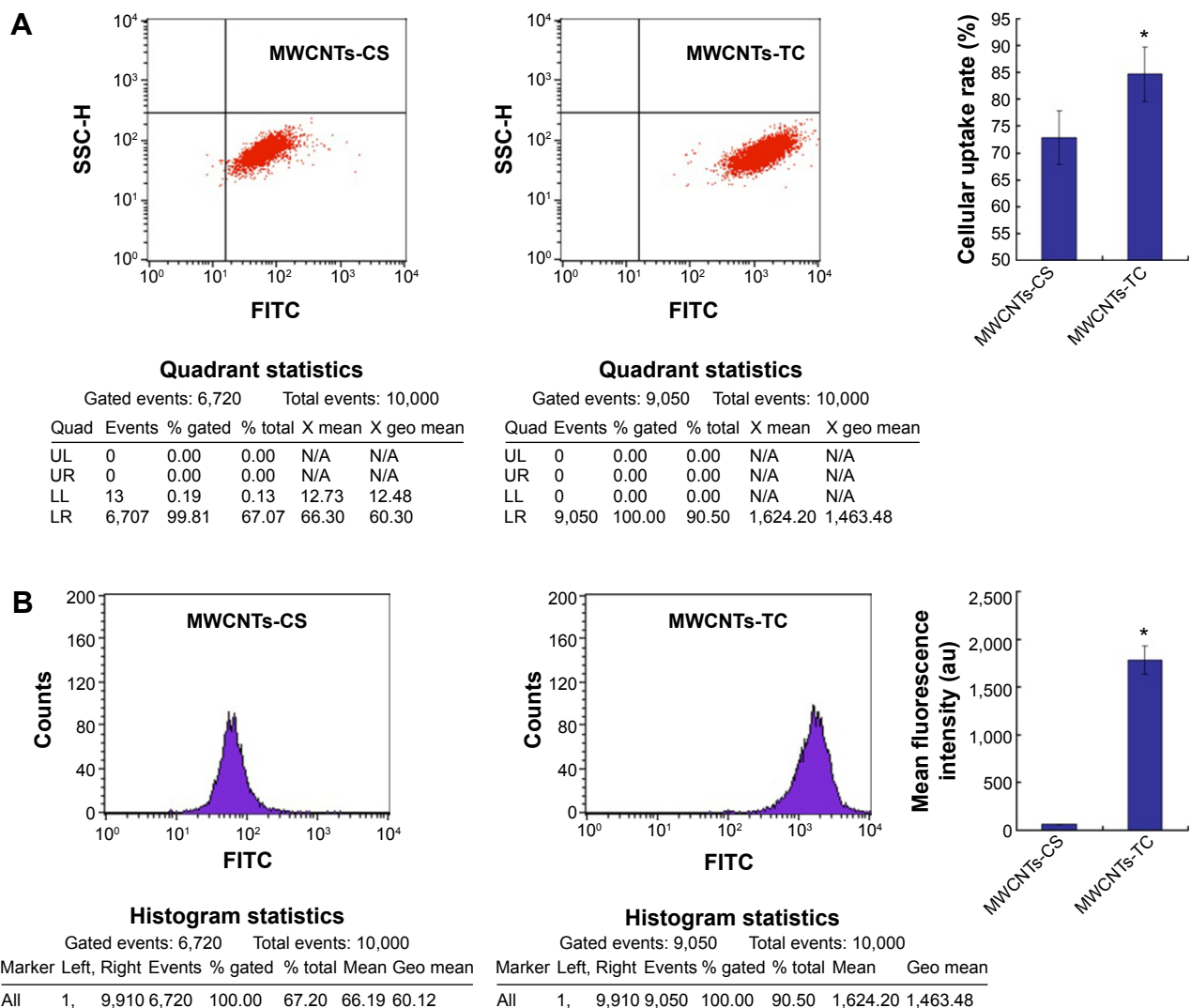


Figure 9 Flow cytometric analysis of cellular uptake.

Notes: (A) Cellular uptake rate; (B) mean fluorescent intensity. * $P < 0.05$ versus MWCNTs-CS.

Abbreviations: MWCNTs-CS, chitosan-conjugated multiwalled carbon nanotubes; MWCNTs-TC, transactivator of transcription–chitosan-conjugated multiwalled carbon nanotubes; FITC, fluorescein isothiocyanate; UL, upper left; UR, upper right; LL, lower left; LR, lower right; geo, geometric mean fluorescence intensity; N/A, not applicable.

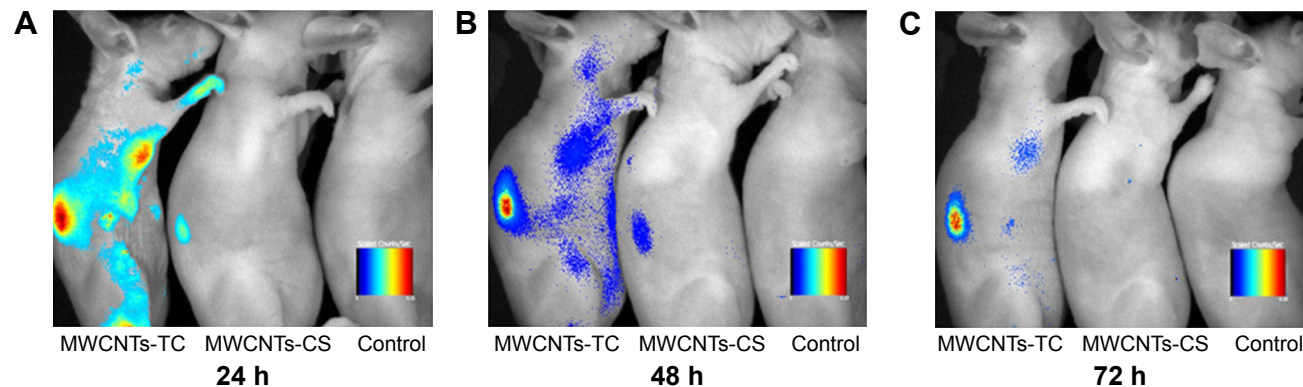


Figure 10 Living animal imaging on breast cancer-bearing mice administered with MWCNTs-TC, MWCNTs-CS, or NS.

Notes: (A) 24 h; (B) 48 h; and (C) 72 h.

Abbreviations: MWCNTs-TC, transactivator of transcription–chitosan-conjugated multiwalled carbon nanotubes; MWCNTs-CS, chitosan-conjugated multiwalled carbon nanotubes; h, hours; NS, normal saline.

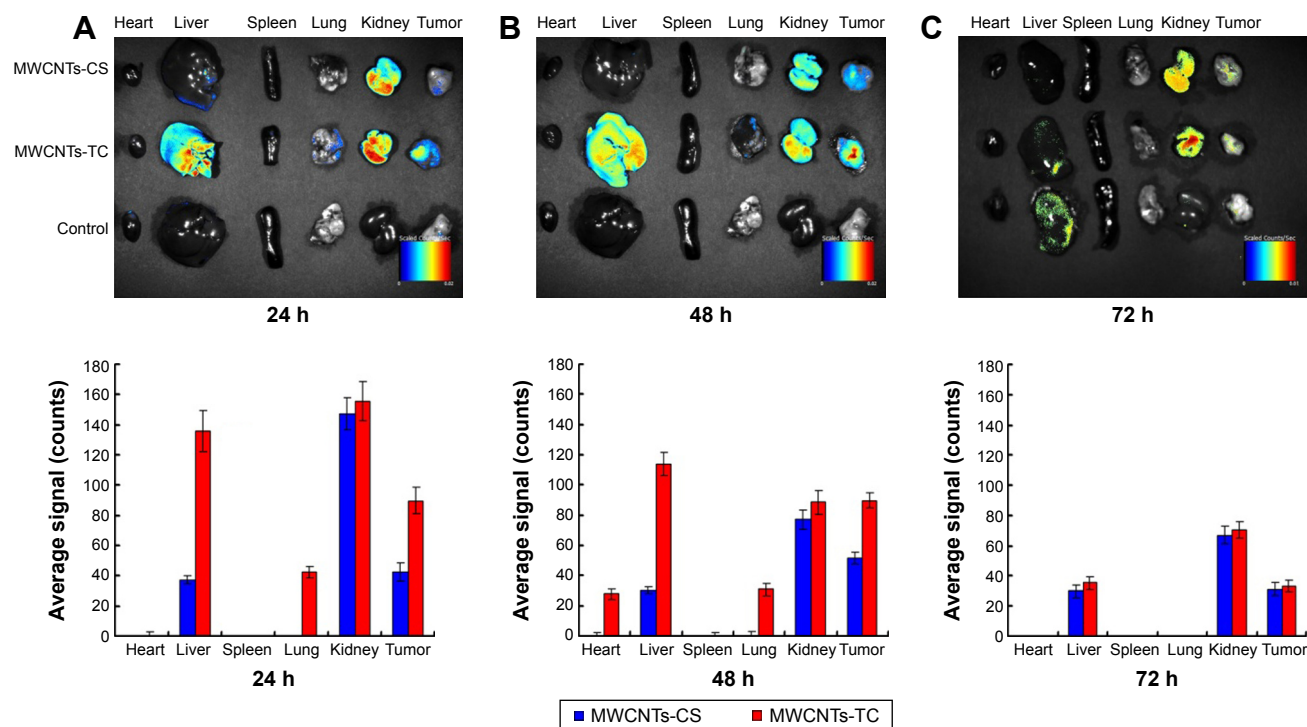


Figure 11 Direct imaging on the excised organs and tissues.

Notes: (A) 24 h; (B) 48 h; and (C) 72 h.

Abbreviations: MWCNTs-CS, chitosan-conjugated multiwalled carbon nanotubes; MWCNTs-TC, transactivator of transcription–chitosan-conjugated multiwalled carbon nanotubes; h, hours.

former. Obviously higher distribution in liver and lung was found in the MWCNTs-TC group as compared with that in the MWCNTs-CS group. The reason is not yet clear as to why MWCNTs-TC were more prone to distribute in the liver and lung as compared with MWCNTs-CS, but this feature might be beneficial for liver- or lung-targeting delivery. Fortunately, no heart distribution was found in either the MWCNTs-CS or MWCNTs-TC group, which would ease the concerns over their heart toxicity. The data also suggested that the kidney pathway was probably the main excretion pathway for both MWCNTs-TC and MWCNTs-CS.

Biosafety is another key concern when designing drug delivery systems. TAT was a peptide derived from the HIV virus, which has been proven to be safe for *in vivo* application.³¹ CS is a widely accepted biodegradable polymer with promising biocompatibility and it has been intensively used as a nonviral drug/gene vector.^{32–34} Therefore, the TC should be considered as a safe material for biomedical application. In the present study, the cytotoxicity of the CNTs against one breast cancer cell line (MD-MBA-231) and two typical cell lines (HUVEC, L929) were evaluated. It was shown that both MWCNTs-TC and MWCNTs-CS were less toxic against the three types of cells as compared with p-MWCNTs, confirming that coating with TC or CS dramatically decreased the

cytotoxicity of the MWCNTs. It was noted, however, that MWCNTs-TC demonstrated slightly higher cytotoxicity than MWCNTs-CS at the same concentration, suggesting that the introduction of the TAT peptide might lead to higher cytotoxicity, probably as the result of the higher amount of MWCNTs-TC taken up by each cell in comparison with that of MWCNTs-CS. Actually, if the amount of the CNTs in each cell was taken into account, MWCNTs-TC should be anticipated to be much less cytotoxic than MWCNTs-CS. When combined with some targeting moieties, MWCNTs-TC might demonstrate much greater potential in killing the tumor cells in comparison to MWCNTs-CS. Also interesting was that the CNTs were more cytotoxic against the normal cell lines (HUVEC and L929) than against the tumor cells, which was in line with the previous observations,³⁵ reflecting the stronger tolerance of cancerous cells against CNT exposure as compared with normal cells.

Conclusion

In conclusion, the preliminary data collected from the present study demonstrated that MWCNTs-TC were essentially nontoxic with perfect water solubility, and they were more efficient in term of cancer-targeted intracellular transport both *in vitro* and *in vivo* as compared with MWCNTs-CS,

suggesting the great potential of MWCNTs-TC in cancer therapy. However, further investigation on drug-loading capacity, targeting specificity, and tumor suppressive effects should be conducted before their application in the clinic.

Acknowledgments

This research was jointly supported by the Natural Science Foundation of Tianjin (grant number: 11JCZDJC20300), the National Natural Science Foundation of China (grant numbers: 81271693 and 31200674), the Peking Union Medical College Youth Fund, and the Fundamental Research Funds for the Central Universities (grant number: 3332013060).

Disclosure

The authors report no conflicts of interest in this work.

References

- Wong BS, Yoong SL, Jagusiak A, et al. Carbon nanotubes for delivery of small molecule drugs. *Adv Drug Deliv Rev*. 2013;65(15):1964–2015.
- Jain KK. Advances in use of functionalized carbon nanotubes for drug design and discovery. *Expert Opin Drug Discov*. 2012;7(11):1029–1037.
- Bates K, Kostarelos K. Carbon nanotubes as vectors for gene therapy: past achievements, present challenges and future goals. *Adv Drug Deliv Rev*. 2013;65(15):2023–2033.
- Gottardi R, Douradinha B. Carbon nanotubes as a novel tool for vaccination against infectious diseases and cancer. *J Nanobiotechnology*. 2013;11:30.
- Jeyamohan P, Hasumura T, Nagaoka Y, Yoshida Y, Maekawa T, Kumar DS. Accelerated killing of cancer cells using a multifunctional single-walled carbon nanotube-based system for targeted drug delivery in combination with photothermal therapy. *Int J Nanomedicine*. 2013;8:2653–2667.
- Kam NW, O'Connell M, Wisdom JA, Dai H. Carbon nanotubes as multifunctional biological transporters and near-infrared agents for selective cancer cell destruction. *Proc Natl Acad Sci U S A*. 2005;102(33):11600–11605.
- Brennan ME, Coleman JN, Drury A, Lahr B, Kobayashi T, Blau WJ. Nonlinear photoluminescence from van Hove singularities in multi-walled carbon nanotubes. *Opt Lett*. 2003;28(4):266–268.
- Torti SV, Byrne F, Whelan O, et al. Thermal ablation therapeutics based on CN(x) multi-walled nanotubes. *Int J Nanomedicine*. 2007;2(4):707–714.
- Zhang W, Guo Z, Huang D, Liu Z, Guo X, Zhong H. Synergistic effect of chemo-photothermal therapy using PEGylated graphene oxide. *Biomaterials*. 2011;32(33):8555–8561.
- Wu W, Li R, Bian X, et al. Covalently combining carbon nanotubes with anticancer agent: preparation and antitumor activity. *ACS Nano*. 2009;3(9):2740–2750.
- Fujigaya T, Yamamoto Y, Kano A, Maruyama A, Nakashima N. Enhanced cell uptake via non-covalent decollation of a single-walled carbon nanotube-DNA hybrid with polyethylene glycol-grafted poly(L-lysine) labeled with an Alexa-dye and its efficient uptake in a cancer cell. *Nanoscale*. 2011;3(10):4352–4358.
- Al-Jamal KT, Toma FM, Yilmazer A, et al. Enhanced cellular internalization and gene silencing with a series of cationic dendron-multiwalled carbon nanotube: siRNA complexes. *FASEB J*. 2010;24(11):4354–4365.
- Lu YJ, Wei KC, Ma CC, Yang SY, Chen JP. Dual targeted delivery of doxorubicin to cancer cells using folate-conjugated magnetic multi-walled carbon nanotubes. *Colloids Surf B Biointerfaces*. 2012;89:1–9.
- Iancu C, Mocan L, Bele C, et al. Enhanced laser thermal ablation for the in vitro treatment of liver cancer by specific delivery of multiwalled carbon nanotubes functionalized with human serum albumin. *Int J Nanomedicine*. 2011;6:129–141.
- Rastogi V, Yadav P, Bhattacharya SS, et al. Carbon nanotubes: an emerging drug carrier for targeting cancer cells. *J Drug Deliv*. 2014;2014:670815.
- Chen Y, Xu Y, Wang Q, Gunasinghe RN, Wang XQ, Pang Y. Highly selective dispersion of carbon nanotubes by using poly(phenyleneethynylene)-guided supermolecular assembly. *Small*. 2013;9(6):870–875.
- Hadidi N, Kobarfard F, Nafissi-Varcheh N, Aboofazeli R. Optimization of single-walled carbon nanotube solubility by noncovalent PEGylation using experimental design methods. *Int J Nanomedicine*. 2011;6:737–746.
- Di Crescenzo A, Ettore V, Fontana A. Non-covalent and reversible functionalization of carbon nanotubes. *Beilstein J Nanotechnol*. 2014;5:1675–1690.
- Vardharajula S, Ali SZ, Tiwari PM, et al. Functionalized carbon nanotubes: biomedical applications. *Int J Nanomedicine*. 2012;7:5361–5374.
- Holt BD, Dahl KN, Islam MF. Quantification of uptake and localization of bovine serum albumin-stabilized single-wall carbon nanotubes in different human cell types. *Small*. 2011;7(16):2348–2355.
- Ghosh S, Dutta S, Gomes E, et al. Increased heating efficiency and selective thermal ablation of malignant tissue with DNA-encased multiwalled carbon nanotubes. *ACS Nano*. 2009;3(9):2667–2673.
- Kato Y, Onishi H, Machida Y. Application of chitin and chitosan derivatives in the pharmaceutical field. *Curr Pharm Biotechnol*. 2003;4(5):303–309.
- Jarmila V, Vavříková E. Chitosan derivatives with antimicrobial, antitumor and antioxidant activities—a review. *Curr Pharm Des*. 2011;17(32):3596–3607.
- Wang JJ, Zeng ZW, Xiao RZ, et al. Recent advances of chitosan nanoparticles as drug carriers. *Int J Nanomedicine*. 2011;6:765–774.
- Hu Q, Li B, Wang M, Shen J. Preparation and characterization of biodegradable chitosan/hydroxyapatite nanocomposite rods via in situ hybridization: a potential material as internal fixation of bone fracture. *Biomaterials*. 2004;25(5):779–785.
- Liao X, Zhang X. Preparation, characterization and cytotoxicity of carbon nanotube-chitosan-phycoerythrin complex. *Nanotechnology*. 2012;23(3):035101.
- Piovesan S, Cox PA, Smith JR, Fatouros DG, Roldo M. Novel biocompatible chitosan decorated single-walled carbon nanotubes (SWNTs) for biomedical applications: theoretical and experimental investigations. *Phys Chem Chem Phys*. 2010;12(48):15636–15643.
- Zhou F, Wu S, Song S, Chen WR, Resasco DE, Xing D. Antitumor immunologically modified carbon nanotubes for photothermal therapy. *Biomaterials*. 2012;33(11):3235–3242.
- Yan CY, Gu JW, Hou DP, et al. Synthesis of Tat tagged and folate modified N-succinyl-chitosan self-assembly nanoparticles as a novel gene vector. *Int J Biol Macromol*. 2015;72:751–756.
- Yuan W, Kuai R, Ran R, et al. Increased delivery of doxorubicin into tumor cells using extracellularly activated TAT functionalized liposomes: in vitro and in vivo study. *J Biomed Nanotechnol*. 2014;10(8):1563–1573.
- Zhang S, Zhao Y, Zhi D, Zhang S. Non-viral vectors for the mediation of RNAi. *Bioorg Chem*. 2012;40(1):10–18.
- Zhang X, Yao J, Zhang L, Fang J, Bian F. Synthesis and characterization of PEG-conjugated quaternized chitosan and its application as a gene vector. *Carbohydr Polym*. 2014;103:566–572.
- Lu H, Dai Y, Lv L, Zhao H. Chitosan-graft-polyethylenimine/DNA nanoparticles as novel non-viral gene delivery vectors targeting osteoarthritis. *PLoS One*. 2014;9(1):e84703.
- Eroglu E, Tiwari PM, Waffo AB, et al. A nonviral pHEMA+chitosan nanosphere-mediated high-efficiency gene delivery system. *Int J Nanomedicine*. 2013;8:1403–1415.
- Sohaebuddin SK, Thevenot PT, Baker D, Eaton JW, Tang L. Nanomaterial cytotoxicity is composition, size, and cell type dependent. *Part Fibre Toxicol*. 2010;7:22.

International Journal of Nanomedicine**Dovepress****Publish your work in this journal**

The International Journal of Nanomedicine is an international, peer-reviewed journal focusing on the application of nanotechnology in diagnostics, therapeutics, and drug delivery systems throughout the biomedical field. This journal is indexed on PubMed Central, MedLine, CAS, SciSearch®, Current Contents®/Clinical Medicine,

Journal Citation Reports/Science Edition, EMBase, Scopus and the Elsevier Bibliographic databases. The manuscript management system is completely online and includes a very quick and fair peer-review system, which is all easy to use. Visit <http://www.dovepress.com/testimonials.php> to read real quotes from published authors.

Submit your manuscript here: <http://www.dovepress.com/international-journal-of-nanomedicine-journal>